

# Electrical Characteristics of the Mars Electrostatic Precipitator

Michael R. Johansen, James R. Phillips III, Jerry J. Wang, Jaysen Mulligan, Paul J. Mackey, Carlos I. Calle

Exploration Research and Technology Programs

NASA Kennedy Space Center

phone: (1) 321-861-2133

e-mail: [michael.r.johansen@nasa.gov](mailto:michael.r.johansen@nasa.gov)

Judson S. Clements

Department of Physics and Astronomy, Appalachian State University

**Abstract**— NASA's next generation Mars missions will include chemical processing plants to convert the Martian atmosphere into consumable products needed to support astronaut activities. The thin, mostly carbon dioxide atmosphere of Mars is estimated to have 5-10 particles/cm<sup>3</sup> which have a radius of 1.6-2.27  $\mu\text{m}$  on average. These dust particles could potentially foul the chemical process or reduce the purity of the products. Electrostatic precipitation is one possible solution to remove dust particles from the ingested Mars atmosphere. The Electrostatics and Surface Physics Laboratory at NASA's Kennedy Space Center has developed an electrostatic precipitator testbed to understand the intricacies of corona discharges in dusty flows simulating Mars atmospheric conditions. Current-voltage trends have been established for a number of precipitator flow conditions. Corona onset voltage and streamer onset voltage trends versus pressure are also established.

## I. INTRODUCTION

Astronauts on next-generation planetary exploration missions will be required to use the resources that are found on-site through a process known as in-situ resource utilization (ISRU). One of the commodities that astronauts will use on Mars is the thin, mostly carbon dioxide atmosphere. The carbon dioxide can be converted to methane for propellant through the Sabatier reaction. Oxygen for breathable air and for rocket fuel oxidizer can be created through solid oxide electrolysis [1].

The top layer of the moon, Mars, and some asteroids are covered with a fine layer of dust. These very fine dust particles are formed by a number of natural processes including meteorite bombardment and particle to particle interaction. On Mars this particle to particle interaction is caused by Martian atmospheric wind. These winds can occasionally produce dust storms that can encompass the entire planet. Even in relatively calm conditions when dust storms are not occurring, the Mars atmosphere is estimated to contain between 5.36-

8.5 particles per cubic centimeter that have a 1.6-2.27  $\mu\text{m}$  radius. [2]. These fine dust particles must first be removed to produce high quality methane and oxygen from the Martian atmosphere and to prevent fouling of the chemical processing plant.

Electrostatic precipitation may be the most feasible option of clearing dust particles from Mars ISRU atmospheric intakes, as traditional media filters may cause an unsatisfactory pressure drop. Terrestrial electrostatic precipitators can have dust cleaning efficiencies greater than 99% and have only minimal pressure drop in a wire-cylinder configuration. However, Mars atmospheric pressure is 6.3 mbar and thus approaches the Paschen minimum for many useful geometries. This prevents Martian electrostatic precipitator geometries from reaching very high potentials that are used in terrestrial electrostatic precipitation. Earlier work in this subject demonstrates that electrostatic precipitation is feasible in a static fluid simulated Martian environment [3], [4]. The Martian Electrostatic Precipitator Testbed (ESP testbed) was developed to study the effectiveness of an electrostatic precipitator in a simulated Mars ISRU flow. This testbed is used to rapidly test a variety of wire-cylinder precipitator geometries. In this paper, we present preliminary experimental results for electrical characteristics of corona discharges in a carbon dioxide flow that simulates Martian ISRU processes.

## II. THEORY

### A. Overview

The electrostatic precipitator geometry investigated here consists of a wire electrode installed coaxially inside of a cylindrical shell electrode that doubles as a vacuum chamber. The void between the two electrodes is filled with a rarified gas containing dust particles and a DC high voltage of either positive or negative polarity is applied to the wire electrode while the outer shell of the precipitator is grounded. This potential difference generates an electric field which interacts with the particles within the system in various ways explored further in the following sections.

### B. Electric Fields

The precipitator operates in two regimes separated by the potential difference required to generate a corona discharge in the gas. This potential is known as the corona onset voltage,  $V_0$ . The electric field within the precipitator produced by potentials below this limit as a function of radial position away from the co-axis of the system,  $r$ , is given by

$$E_0(r) = \frac{V}{r \ln\left(\frac{r_p}{r_w}\right)}, \quad V \leq V_0 \quad (1)$$

where  $r_p$  is the inner radius of the precipitator wall,  $r_w$  is the radius of the wire electrode, and  $V$  is the voltage applied to the wire electrode [Cross, Eq 7.122]. At potentials above the corona onset voltage, gas molecules within the precipitator become ionized and electron/ion pairs are generated within the gas. These charged particles allow the gas to conduct, which modifies the electric field to become

$$E(r) = \sqrt{\frac{I}{2\pi\epsilon_0 b l_p} + \left(\frac{r_w}{r}\right)^2 \left(E_0^2 - \frac{I}{2\pi\epsilon_0 b l_p}\right)}, \quad V > V_0 \quad (2)$$

where  $l_p$  is the precipitator length,  $I$  is the corona current,  $b$  is the ion mobility of the gas, and  $\epsilon_0$  is the vacuum permittivity [Cross, Eq 7.124]. This corona discharge is capable of charging the particles within the precipitator via two primary mechanisms: corona field charging and thermal diffusion charging.

### C. Corona Field Charging

The corona field charging mechanism relies on the charged particles generated by the corona being accelerated by the applied electric field and depositing on dust particles within the precipitator. The saturation charge of a particle in a given electric field is a function of the magnitude of the field at the surface of the particle (unmodified by any fields generated by the charges on the surface of the particle in question) and is expressed as

$$q_s(r) = 12\pi a^2 \frac{\epsilon_0 \epsilon_r}{\epsilon_r + 2} E(r) \quad (3)$$

where  $a$  is the radius of the particle and  $\epsilon_r$  is the relative permittivity of the particle [Cross, Eq 2.13]. The charging rate is described by

$$\frac{dq(r, t)}{dt} = q_s(r) \frac{N_0 e b}{4\epsilon_0} \left[1 - \frac{q(r, t)}{q_s(r)}\right]^2 = q_s(r) \frac{J(r)}{4\epsilon_0 E(r)} \left[1 - \frac{q(r, t)}{q_s(r)}\right]^2 \quad (4)$$

where  $N_0$  is the number of ions per unit volume,  $e$  is the elementary charge,  $J$  is the current density, and  $J(r) = N_0 e b E(r)$  [Cross, Eq 2.21]. Integrating this expression yields the time dependence of the accumulation of charge and is given by

$$q(r, t) = q_s(r) \left[1 + \frac{4\epsilon_0}{N_0 e b t}\right]^{-1} = q_s(r) \left[1 + \frac{4\epsilon_0 E(r)}{J(r) t}\right]^{-1} = q_s(r) \left(1 + \frac{\tau}{t}\right)^{-1} \quad (5)$$

where  $\tau$  is the time constant describing time required for a particle to reach half of its saturation charge [Cross, Eq 2.14]. Combining Eq. 3 and Eq.5 yields the complete time dependent charging expression of

$$\begin{aligned} q(r, t) &= 12\pi a^2 \frac{\epsilon_0 \epsilon_r}{\epsilon_r + 2} E(r) \left[1 + \frac{4\epsilon_0}{N_0 e b t}\right]^{-1} \\ &= 12\pi a^2 \frac{\epsilon_0 \epsilon_r}{\epsilon_r + 2} E(r) \left[1 + \frac{4\epsilon_0 E(r)}{J(r) t}\right]^{-1} \end{aligned} \quad (6)$$

which depends quadratically on the particle radius and linearly on the electric field.

#### D. Thermal Diffusion Charging

The thermal diffusion charging mechanism relies on thermal collisions between the charged particles generated by the corona discharge and the dust particles within the precipitator. In order for a dust particle to accumulate charge via this method of charging, an ion in the gas with sufficient energy to overcome the Coulomb interaction will need to collide with the particle. The Boltzmann distribution determining the number of ions in a sufficiently energetic state to satisfy this condition is given by

$$N = N_0 \exp\left(-\frac{W}{k_B T}\right) = N_0 \exp\left(-\frac{1}{4\pi\epsilon_0} \frac{1}{k_B T} \frac{qe}{a}\right) \quad (7)$$

where  $N$  and  $N_0$  are the number densities of the excited ions and all ions in the gas, respectively,  $T$  is the gas temperature,  $e$  is the elementary charge (due to gas molecules being singly ionized),  $W$  is the energy to overcome the Coulomb repulsion between an ion and a dust particle with radius,  $a$ , and charge,  $q$ , and  $k_B$  is the Boltzmann constant [Cross, Eq 2.24]. The charging rate is given by the flux of incident charged ions on the surface area,  $A_p$ , of the dust particle as such

$$\begin{aligned} \frac{dq(r, t)}{dt} &= A_p N e u(r) = \pi a^2 e u(r) N_0 \exp\left(-\frac{1}{4\pi\epsilon_0} \frac{1}{k_B T} \frac{qe}{a}\right) \\ &= \pi a^2 J(r) \exp\left(-\frac{1}{4\pi\epsilon_0} \frac{1}{k_B T} \frac{qe}{a}\right) \end{aligned} \quad (8)$$

where  $u$  is the ion drift velocity and  $J(r) = N_0 e u(r)$ . Upon integrating, the time dependent expression for the particle charge is found to be

$$\begin{aligned} q(r, t) &= \frac{4\pi\epsilon_0 k_B T}{e} a \ln \left[ 1 + \frac{N_0 e^2 u(r)}{4\epsilon_0 k_B T} at \right] \\ &= \frac{4\pi\epsilon_0 k_B T}{e} a \ln \left[ 1 + \frac{eJ(r)}{4\epsilon_0 k_B T} at \right] \end{aligned} \quad (9)$$

which depends logarithmically on the particle size and is independent of the electric field [Cross, Eq 2.26].

#### E. Mixed Mode Charging

The dependence of particle radius on dust particle charge during corona field charging (Eq. 6) is quadratic, while during thermal diffusion charging (Eq.9) is logarithmic. Because of this, thermal diffusion charging dominates for small particle size, while corona field charging dominates for large particle size. For particles of intermediate size, both mechanisms

must be considered by summing the two charging rates Eq. 4 and Eq. 8 [4], and integrating to find the time dependence of the total charge on the particle [5].

#### F. Current Voltage Relationship

For a given precipitator geometry flowing a gas with known properties, the electric field expressed in Eq. 2 becomes a function of applied wire electrode voltage and current flowing out of the precipitator to ground. In order to simplify the relationship to a single equation with one unknown, rather than two, it is important to characterize the current draw of the system over a range of applied voltages. With this information, it is possible to determine the electric field at every radial position within the precipitator.

Similarly, the expressions found for the charge on the dust particles shown in Eq. 6 and Eq. 9 depend on the properties of the particles, properties of the gas, applied wire electrode voltage and current flowing out of the precipitator to ground. For a given type of dust particle with known size and permittivity, the charging characteristics of the dust may be determined from the relationship between the current draw of the system over a range of applied voltages.

### III. EXPERIMENTAL RESULTS

The ESP testbed was developed to characterize the physics of corona discharge in the Martian environment. This testbed as shown in Fig. 1. The testbed consists of a stainless steel tube that is 1 m long and has an inner diameter of 7.1 cm. A wire with diameter of 125  $\mu\text{m}$  was used as the high voltage electrode to generate the charging mechanism. The wire is suspended at the center of the stainless steel tube. The testbed uses a combination of an upstream flow controller and a downstream pressure controller to maintain an average Martian pressure of 4.75 torr. The testbed is capable of generating volumetric flow rate up to 2 SLPM using the described setup.

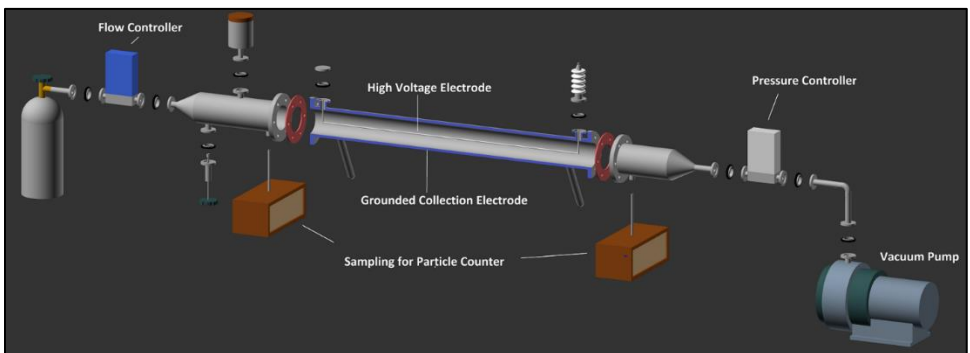


Fig. 1 – Electrostatic precipitator expanded view. Particle sampling of the electrostatic precipitator occurs in both upstream and downstream locations to have continuous particle collection efficiency data.

One of the important aspects of the charging mechanism is the current-voltage relationship (IV curve). By determining the corona current at a given voltage, the efficiency of a precipitator with a prescribed geometry can be calculated. The composite of Mars atmosphere contains carbon dioxide, argon, nitrogen, oxygen, and other trace gases. Previous studies

have indicated that carbon dioxide is a good substitute for experimental purposes [6]. Since the behavior of the IV curve is heavily dependent of the gas properties and species, a comparison experiment to validate earlier findings was conducted with carbon dioxide and a gas that more closely resembles Martian atmospheric composition. As shown in Fig. 2, the Mars gas and CO<sub>2</sub> gas produced similar IV curves at a range of pressure between 4.75 torr to 7.00 torr.

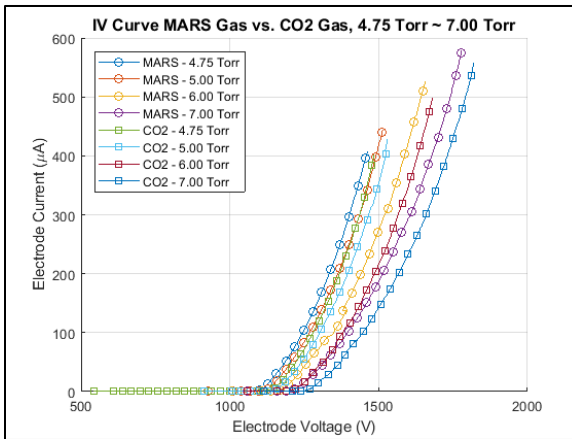


Fig. 2. – Current-voltage relationships for 1 7.1 cm cylinder with a 125  $\mu\text{m}$  wire. As expected, the corona onset voltage increases as well as the streamer onset voltage with increased pressure.

In order to support astronaut activities in future Mars missions, the ESP needs to expand in size to accommodate for the increase in volumetric flow rate. The ESP testbed is capable of injecting 2000 standard cubic centimeter per minute (SCCM) of CO<sub>2</sub> while a volumetric flow rate to support human mission is estimated at 550 L/min. To better understand the behavior of the corona as the geometry of the ESP expands to meet the operating requirement, IV curve tests were performed at different pressure with incremental flow rate. As shown in Fig. 3 and Fig. 4, the increase in flow rate did not change the IV curve. The corona onset voltage and streamer “breakdown” voltage remained consistent as the flow rate increased at different pressure level. The stable corona regime was also consistent as the flow rate increased. The consistency of stable IV curve in different flow rate indicated that for the ESP to support future human mission on Mars, the current setup can be expanded in parallel to increase the volumetric flow rate while maintaining a certain cross-sectional area and length.

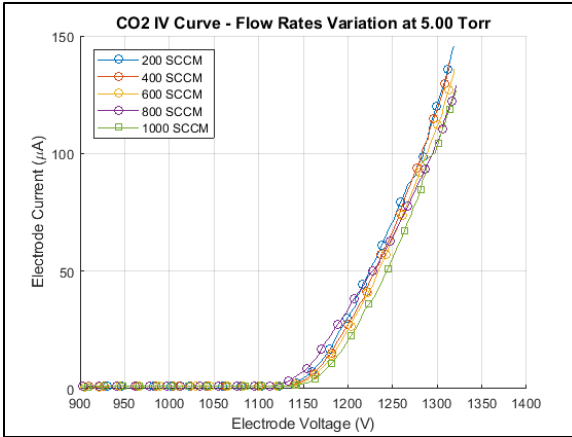


Fig. 3 – Current voltage relationship for a 7.1 cm diameter cylinder with a coaxial 125  $\mu\text{m}$  wire. There is minimal impact in the relationship due to increased flow rate at 5 torr.

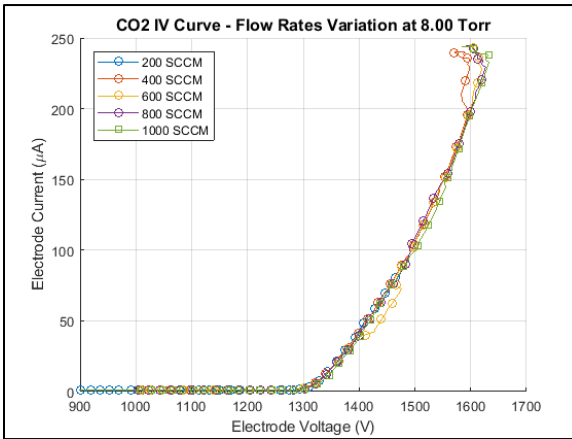


Fig. 4 – Current voltage relationship for a 7.1 cm diameter cylinder with a coaxial 125  $\mu\text{m}$  wire. There is minimal impact in the relationship due to increased flow rate at 8 torr.

Using the IV data shown in Fig. 2 the onset voltage and streamer voltage were determined for the precipitator geometry of 7.1 cm in inner diameter and 125  $\mu\text{m}$  diameter electrode. The onset and breakdown voltages increased as the pressure of the test section increased. In this particular setup, a positive corona was used instead of a negative. Although a negative corona provides a more stable IV regime at atmospheric pressure air, the stable negative IV regime in low pressure CO<sub>2</sub> is narrow; making consistent particle charging difficult if the pressure fluctuates. In contrast, a positive corona in low pressure CO<sub>2</sub> yielded a larger stable IV regime that provided a better operating margin for consistent particle charging.

#### IV. FUTURE WORK

A variety of high voltage and ground electrodes will be tested under Mars atmospheric composition and pressure to develop corona onset and streamer onset trends. Other trends,

such as the concavity of the current-voltage relationship, will also be investigated. Simulated Martian dust will be incorporated into these experiments to quantify coronal electrical property changes in dusty Martian flows. These trends will be used to optimize the geometry of a Martian electrostatic precipitator which may operate someday on the red planet.

## REFERENCES

- [1] G. Sanders, "Current NASA Plans for Mars In Situ Resource Utilization," 2018.
- [2] J. R. Phillips III, J. R. Pollard, M. R. Johansen, P. J. Mackey, J. S. Clements and C. I. Calle, "Martian Atmospheric Dust Mitigation for ISRU Intakes via Electrostatic Precipitation," in *ASCE Earth and Space*, Orlando, Florida, 2016.
- [3] C. I. Calle, M. R. Johansen, B. S. Williams, M. D. Hogue, P. J. Mackey and J. S. Clements, "Dust Removal Technology for a Mars In Situ Resource Utilization System," in *AIAA Space Conference and Exposition*, Long Beach, California, 2011.
- [4] J. S. Clements, S. M. Thompson, N. D. Cox, M. R. Johansen, B. S. Williams, M. D. Hogue, M. L. Lowder and C. I. Calle, "Development of an Electrostatic Precipitator to Remove Martian Atmospheric Dust From ISRU Gas Intakes During Planetary Exploration Missions," *IEEE Transactions on Industry Applications*, pp. 2388-2396, 2013.
- [5] S. Oglesby and G. B. Nichols, "A Manual of Electrostatic Precipitator Technology Part 1 - Fundamentals," Southern Research Institute, Birmingham, Alabama, 1970.
- [6] C. I. Calle, J. S. Clements, J. Willis and C. R. Buhler, "Paschen Breakdown Experiments in a Martian Atmosphere," *NASA Technical Memorandum 2004-2/1535*, pp. 86-87, 2004.
- [7] J. Cross, *Electrostatics: Principles, Problems, and Applications*, CRC Press, 1987.